are not likely to be directly affected by surface chemical effects. The recombination lifetime of electrons at the semiconductor surface is critical to the kinetics of photocatalytic reductions. This lifetime can be increased by the presence of hole-acceptor surface states which are themselves inefficient recombination centers.[33] Adsorbed hydroxide could form such surface states. The quantum efficiency for reduction would then increase with the surface hydroxide concentration which, under steady-state conditions, depends on the rate of surface rehydroxylation. Hydroxide-induced band bending and inhibition of recombination at the surface probably both play a role in the kinetics of photoelectrochemical cells operated at zero applied potential, where band bending is marginal. Careful experiments in which light intensity, electrolyte pH, and (for electrochemical cells) applied potential are systematically varied may be able to further elucidate the kinetic roles of hydroxide.

In summary, electrolyte hydroxide concentration has been found to be important to the rate of hydrogen photoproduction on platinized and metal-free $SrTiO_3$ crystals. Hydroxide ions may be directly involved in a rate-limiting step, such as the production of active surface hydroxyl groups. Such an interpretation of our results in aqueous electrolyte is in agreement with reports that surface hydroxyl groups play a crucial role in semiconductor photochemistry at the gas-solid interface.[8,26,27]

4. Gas-Phase Considerations. We could measure no hydrogen production from platinized or metal-free $SrTiO_3$ crystals illuminated in water vapor at a pressure of about 20 Torr. Hydrogen production rates as low as 12 monolayers/h could have been unequivocally detected. The same crystals coated with basic deliquescent compounds, saturated with water vapor, and illuminated yielded hydrogen at readily measurable rates.

Schrauzer and Guth[7] have reported the photodissociation of water on TiO_2 powders. However, the process stopped within several hours and could not be sustained to produce catalytic amounts of hydrogen. As discussed in the Experimental Section, product yields, to serve as a criterion for catalytic activity, should be normalized to the total surface area of the catalyst. Using the high end of their reported 0.5-1-μm particle size range and assuming spherical particles, they observed the maximum hydrogen accumulation corresponding to ~two monolayers.

The ion-transport problems associated with photoelectrochemical reactions in the gas phase have already been discussed. We have, however, demonstrated that UV-illuminated metal-free $SrTiO_3$ crystals in aqueous alkaline solution can evolve thousands of monolayers of hydrogen by a photocatalytic mechanism in which all chemistry occurs on the illuminated semiconductor surface. This finding lends support to the argument advanced by Van Damme and Hall[8] that some surface chemical problem, rather than problems with the delivery of photogenerated electrons and holes to the semiconductor surface, has restricted the yield of photoreactions at the gas-solid interface to one monolayer or less. The hydroxide dependence of the liquid-phase photocatalytic reaction lends some support to their contention that the yield of the gas-phase reaction is limited by an inability to rehyroxylate the surface with water vapor. Development of techniques for the facile rehydroxylation of oxide semiconductor surfaces may prove a key to sustainable photocatalytic water dissociation at the gas-solid interface.

Acknowledgments. This work was supported by the Division of Chemical Sciences, Office of Basic Energy Sciences, U.S. Department of Energy, under Contract S-7405-ENG-48. F.T.W. was supported under a NSF Graduate Fellowship.

(33) P. Vohl, *Photogr. Sci. Eng.*, **13**, 120 (1969).

Crystal Structure and Conformation of the Cyclic Trimer of a Repeat Pentapeptide of Elastin, *cyclo*-(L-Valyl-L-prolylglycyl-L-valylglycyl)$_3$

William J. Cook,*[1,3,4] Howard Einspahr,[2-4] Tina L. Trapane,[5] Dan W. Urry,[2,5] and Charles E. Bugg[2-4]

Contribution from the Department of Pathology, Department of Biochemistry, Comprehensive Cancer Center, Institute of Dental Research, and Laboratory of Molecular Biophysics, University of Alabama in Birmingham, University Station, Birmingham, Alabama 35294.
Received January 31, 1980

Abstract: X-ray diffraction data were used to determine the crystal structure of *cyclo*-(L-Val-L-Pro-Gly-L-Val-Gly)$_3$, the cyclic trimer of a repeat pentapeptide of elastin. The crystals are trigonal, space group $R3$, but are described by using a triply primitive hexagonal unit cell with a = 28.474 (1) and c = 10.044 (1) Å. Intensity data for 2565 independent reflections were measured with an automated diffractometer. The structure was solved by direct methods and refined by least squares to R = 0.109. The cyclic pentadecapeptide consists of three β(II) turns joined by Val-Gly-Val bridges. Hydrophilic and hydrophobic channels that run parallel to the c axis are formed by the stacking of cyclic peptides on threefold axes.

Introduction

Tropoelastin, the soluble precursor protein of fibrous elastin, contains in its sequence several stretches of repeating oligopeptides. The three main repeating oligopeptides are a tetrapeptide, Val$^{(1)}$-Pro$^{(2)}$-Gly$^{(3)}$-Gly$^{(4)}$, a pentapeptide, Val$^{(1)}$-Pro$^{(2)}$-Gly$^{(3)}$-Val$^{(4)}$-Gly$^{(5)}$, and a hexapeptide, Ala$^{(1)}$-Pro$^{(2)}$-Gly$^{(3)}$-Val$^{(4)}$-Gly$^{(5)}$-Val$^{(6)}$.[6a,b] Nuclear magnetic resonance (NMR) studies have shown that the repeated-oligopeptide segments of elastin are

(1) Department of Pathology.
(2) Department of Biochemistry.
(3) Comprehensive Cancer Center.
(4) Institute of Dental Research.
(5) Laboratory of Molecular Biophysics.

(6) (a) Foster, J. A.; Bruenger, E.; Gray, W. R.; Sandberg, L. B. *J. Biol. Chem.* **1973**, *248*, 2876-2879. (b) Gray, W. R.; Sandberg, L. B.; Foster, J. A. *Nature (London)* **1973**, *246*, 461-466. (c) Urry, D. W.; Long, M. M. *CRC Crit. Rev. Biochem.* **1976**, *4*, 1-45. (d) Urry, D. W.; Trapane, T. L.; Sugano, H., in preparation.

0002-7863/80/1502-5502$01.00/0

Table I. Crystal Data

stoichiometry	$C_{57}H_{90}O_{15}N_{15}\cdot 1.2C_3H_6O\cdot 5.7H_2O$
Z	3
space group	$R3$
a	28.474 (1) Å
c	10.044 (1) Å
ρ(calcd)	1.006 g cm^{-3}
ρ(obsd)	1.19 g cm^{-3}
μ (Cu K$\bar{\alpha}$)	8.2 cm^{-1}

comprised of subunits that are conformationally equivalent within the NMR time scale; on the basis of NMR, ultraviolet, and circular dichroism spectroscopic studies, several secondary structural elements have been proposed as features of one or more of these repeated-peptide segments.[6c] The conformational feature common to all three repeated-peptide segments is a β(II) turn that includes a ten-atom hydrogen-bonded ring formed by a residue-1 C–O···H–N residue-4 hydrogen bond. Another secondary structural feature that is associated with the pentapeptide and hexapeptide segments in some solvent systems is an 11-atom hydrogen-bonded ring involving a Gly$^{(3)}$N–H···O–C Gly$^{(5)}$ hydrogen bond. Also, the tetramer and pentamer units in chloroform, as well as high polymers of these units in water at elevated temperatures, appear to form a 14-atom hydrogen-bonded ring involving the Val$^{(1)}$ NH and the residue-4 C–O.

In order to further study the conformational properties of these repeating sequences, cyclic peptides composed of oligomers of the repeated pentapeptide have been synthesized. It was felt that a cyclic structure composed of a small number of repeated peptides might closely approximate the conformation of a single turn of the helical structure assumed for the segment. In this regard, the cyclic pentadeca- and eicosapeptides have been examined by NMR and are found to contain secondary structural features, and to show temperature and solvent response, that closely match those of the linear polypentapeptide.[6d] We report here the crystal and molecular structure of the cyclic pentadecapeptide *cyclo*-(Val-Pro-Gly-Val-Gly)$_3$.

Experimental Section

Crystals of *cyclo*-(Val-Pro-Gly-Val-Gly)$_3$ in the form of clear, trigonal prisms were obtained at room temperature from a solution containing Me_2SO, D_2O, and excess methanol. Oscillation and Weissenberg photographs show the crystals to be trigonal with Laue group $\bar{3}$; space group $R3$ is specified by the systematic absence of reflections hkl with $-h + k + l \neq 3n$ (corresponding to the obverse setting) when indexed by using hexagonal axes. The experimental density of 1.19 (5) g cm^{-3} indicates that there are three cyclic pentadecapeptides per triply primitive, hexagonal unit cell and hence that each cyclic peptide lies on a crystallographic threefold axis. The crystal selected for data collection was approximately 0.55 mm long and 0.35 mm on a side. It was sealed in a glass capillary which also contained a small amount of mother liquor to retard crystal deterioration. Approximate cell parameters for use in collection of intensity data were calculated by a least-squares analysis of the angular settings for several medium-angle reflections (Cu K$\bar{\alpha}$, λ = 1.5418 Å) measured on a Picker FACS-1 diffractometer. Intensity data were collected with the diffractometer by the use of a θ–2θ scanning technique. The base scan range of 2° was augmented to account for α_1–α_2 splitting, the scan speed was 2°/min, and the background was counted for 20 s at each terminus of the scans. Measurements were made for each of the 2565 independent reflections with $2\theta < 128°$. Three reference reflections, measured every 100 reflections, lost about 6% of their initial intensity values during the course of data collection. More precise values for the unit-cell parameters were determined immediately after data collection by a least-squares analysis of 2θ values for 15 medium-angle reflections (Cu Kα). These cell parameters, which were used for all subsequent calculations, are not significantly different from those obtained prior to data collection; they are listed in Table I together with other crystal data. The corresponding primitive rhombohedral cell has dimensions of a = 16.777 Å and α = 116.12°.

Reflections with scan counts below background levels were given their calculated negative intensity values and were retained in all subsequent calculations. The intensities were assigned variances, $\sigma^2(I)$, according to the statistics of the scan and background counts plus a correction term $(0.03S)^2$, S being the scan count. Of the 2565 independent intensities, 2020 have $I > \sigma(I)$. Intensities and their variances were corrected for Lorentz and polarization factors, and absorption corrections were applied by using the computer program ORABS.[7a] The data were scaled by means of a Wilson[7b] plot.

The trial structure was obtained with the computer program package MULTAN 78.[7c] Sixteen phase sets were generated for 260 normalized structure factors ($|E| > 1.52$), based on a starting set of five reflections; 3563 triples were utilized in the phase-determining process. The E map computed from the phase set with the lowest ψ_0 figure of merit revealed the 20 atoms comprising the peptide backbone. The side-chain atoms were located in an electron-density map phased on these atoms. One Me_2SO molecule and six water molecules, all with fractional occupancies, were added to the model by means of successive least-squares cycles and difference Fourier syntheses. The difficulties associated with the high correlation between occupancy and thermal parameters of solvent atoms were avoided by assigning occupancies for these atoms based on peak heights in the difference Fourier maps, and holding these occupancies constant during the refinement; the Me_2SO molecule was assigned an occupancy of 0.4, and the water molecules W1–W6 were assigned values of 0.5, 0.4, 0.3, 0.3, 0.2, and 0.2, respectively. During refinement it became evident that F_c values greatly exceeded the F_o values for the reflections at low 2θ, such as might be expected for crystals containing a significant amount of disordered solvent.[8] During the final stages of refinement, the 19 reflections with $2\theta < 20°$ were excluded from least-squares and R-factor calculations.

Positions for the 19 nonmethyl hydrogens asociated with the peptide molecule were calculated by using standard distances and angles. These atoms were included in the calculation of structure factors, but not in the least-squares refinement, and were assigned the isotropic temperature factors of the atoms to which they are bonded. The least-squares calculations were made with a modified version of the full-matrix program ORFLS,[9,10] which minimizes $\sum w(F_o^2 - F_c^2/k^2)^2$, where k is a scale factor and w, the weight, is equal to $1/\sigma^2(F_o^2)$. Scattering factors and anomalous dispersion corrections were from Tables 2.2A, 2.2C, and 2.3.1 of Volume IV of the "International Tables for X-ray Crystallography".[11] The final R index ($\sum||F_o| - |F_c||/\sum|F_o|$) is 0.109, and the goodness of fit ($[\sum w(F_o^2 - F_c^2)^2/(m - s)]^{1/2}$, where m is the number of reflections used and s is the number of parameters refined) is 2.64. During the last cycle of refinement, no parameter shifted more than one-fifth of its estimated standard deviation. A final difference Fourier map showed no peaks greater than 0.30 e/Å^3. The disparity between F_o and F_c values at low 2θ suggests that some solvent, largely disordered, remains unaccounted for in the final model. The experimental density suggests that this deficit is of the order of about five water molecules per asymmetric unit. We refrained from further attempts to position solvent in this structure because we felt that we had reached the limit of detection for these data.

Results and Discussion

Table II contains the positional parameters and estimated standard deviations for nonhydrogen atoms. Estimated errors in positional coordinates are 0.01 Å for atoms in the cyclic peptide and 0.04 Å for solvent molecules. Table III lists the calculated coordinates of the nonmethyl hydrogen atoms.

Bond distances and angles for the pentapeptide monomer are shown in Figure 1. The characteristic bond distances in the peptide backbone averaged over the five linkages are 1.44 (3) Å for N_i–C_i^α, 1.49 (3) Å for C_i^α–C_i, 1.22 (2) Å for C_i–O_i, and 1.35 (2) Å for C_i–N_{i+1}. These values compare favorably with those reported previously,[12,13] as do the averaged values of the characteristic angles: 113 (3)° for N_i–C_i^α–C_i, 122 (1)° for C_i^α–C_i–O_i, 117 (2)° for C_i^α–C_i–N_{i+1}, 121 (1)° for O_i–C_i–N_{i+1}, and 122 (2)° for C_i–N_{i+1}–$C_i^\alpha{}_{+1}$. The large thermal ellipsoids and, presumably,

(7) (a) Wehe, D. J.; Busing, W. R.; Levy, H. A. "ORABS, a Fortran Program for Calculating Single Crystal Absorption Corrections", Report ORNL-TM-229; Oak Ridge National Laboratory: Oak Ridge, Tenn., 1962. (b) Wilson, A. J. C. *Nature (London)* **1942**, *150*, 151–152. (c) Main, P.; Hull, S. E.; Lessinger, L.; Germain, G.; Declercq, J. P.; Woolfson, M. M. "MULTAN 78, a System of Computer Programs for the Automatic Solution of Crystal Structures from X-ray Diffraction Data", University of York: York, England.
(8) Bragg, W. L.; Perutz, M. F. *Acta Crystallogr.* **1952**, *5*, 277–283.
(9) Busing, W. R.; Martin, K. O.; Levy, H. A. "ORFLS, a Fortran Crystallographic Least-Squares Program", Report ORNL-TM-305; Oak Ridge National Laboratory: Oak Ridge, Tenn., 1962.
(10) Busing, W. R. *Acta Crystallogr., Sect. A.*, **1971**, *27*, 683–684.
(11) "International Tables for X-ray Crystallography", Vol. IV; Kynoch Press: Birmingham, England, 1974.
(12) Marsh, R. E.; Donohue, J. *Adv. Protein Chem.* **1967**, *22*, 235–256.
(13) Ramachandran, E. N.; Kolaskar, A. S.; Ramakrishnan, C.; Sasisekharan, V. *Biochim. Biophys. Acta* **1974**, *359*, 298–302.

Table II. Positional Parameters of Nonhydrogen Atoms[a]

atom	10^4x	10^4y	10^3z
N1	1955 (3)	9890 (3)	517 (1)
C1A	2064 (4)	9527 (4)	446 (1)
C1B	2075 (4)	9105 (4)	544 (1)
C1C	2205 (4)	8697 (4)	474 (1)
C1D	2487 (4)	9394 (5)	654 (1)
C1	1666 (4)	9240 (3)	338 (1)
O1	1185 (3)	9008 (2)	359 (1)
N2	1854 (3)	9239 (3)	213 (1)
C2A	1470 (3)	8935 (4)	106 (1)
C2B	1838 (4)	8982 (5)	−9 (1)
C2C	2355 (4)	9509 (5)	14 (1)
C2D	2413 (3)	9549 (4)	164 (1)
C2	1104 (4)	8365 (4)	144 (1)
O2	1265 (2)	8080 (2)	197 (1)
N3	579 (2)	8159 (3)	104 (1)
C3A	164 (4)	7594 (4)	123 (1)
C3	−107 (4)	7445 (4)	250
O3	−501 (3)	7000 (3)	268 (1)
N4	74 (3)	7820 (3)	351 (1)
C4A	−141 (3)	7710 (3)	482 (1)
C4B	318 (4)	7885 (4)	587 (1)
C4C	618 (5)	7550 (5)	560 (2)
C4D	67 (5)	7766 (6)	728 (1)
C4	−444 (4)	8023 (4)	508 (1)
O4	−207 (3)	8508 (3)	507 (1)
N5	−967 (3)	7731 (3)	536 (1)
C5A	−1275 (4)	7977 (4)	574 (1)
C5	−1754 (4)	7833 (4)	485 (1)
O5	−1870 (3)	7517 (3)	390 (1)
S	−1390 (5)	8060 (5)	78 (1)
OS	−1097 (13)	8217 (13)	−51 (3)
C1S	−1252 (11)	7493 (10)	154 (3)
C2S	−1083 (13)	8627 (13)	183 (3)
W1	283 (7)	8896 (8)	−22 (2)
W2	1370 (8)	9652 (8)	779 (2)
W3	941 (13)	9368 (13)	682 (4)
W4	668 (13)	9430 (12)	541 (3)
W5	−369 (22)	8924 (21)	−194 (5)
W6	382 (18)	9272 (19)	277 (4)

[a] A = α, B = β, C = γ, D = δ; the z coordinate for C3 was not refined.

Table III. Calculated Coordinates of Hydrogen Atoms

atom	10^3x	10^3y	10^3z
H-N1	169	976	591
H-C1A	242	972	402
H-C1B	173	892	589
H-C2A	128	912	83
H1-C2B	191	867	−2
H2-C2B	169	896	−91
H1-C2C	267	950	−29
H2-C2C	234	980	−17
H1-C2D	262	988	198
H2-C2D	262	934	194
H-N3	47	840	64
H1-C3A	−9	751	51
H2-C3A	35	740	109
H-N4	35	818	333
H-C4A	−37	733	492
H-C4B	57	827	576
H-N5	−113	735	522
H1-C5A	−143	782	663
H2-C5A	−108	834	581

the long distance C4B–C4C may be partially due to the fact that methyl hydrogen atoms for the valine residues were not taken into account in the refinement. By all other criteria, however, the residue dimensions and conformations appear well described. H atoms are arranged in trans conformations about both valine C^{α}–C^{β} bonds. The proline ring is in the twisted conformation, the C2B–C2C bond making an angle of 28° with the plane defined by atoms N2, C2A, and C2D; C2B is 0.29 Å above and C2C is 0.25 Å below this plane.

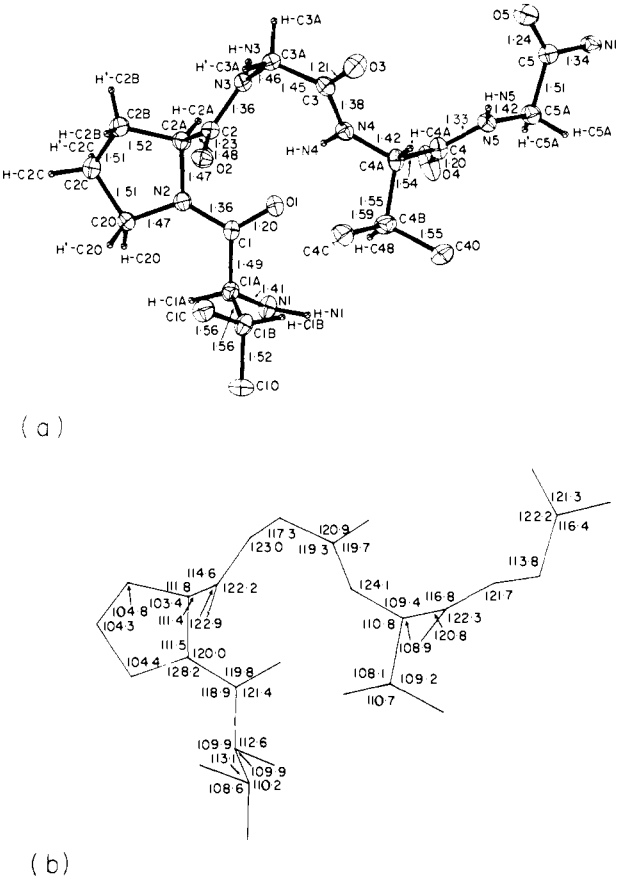

Figure 1. Conformation and dimensions of the pentapeptide monomer. Nonhydrogen atoms are represented by thermal ellipsoids defined by the principal axes of thermal vibration and scaled to include 10% probability. Hydrogen atoms are represented by spheres of 0.1-Å radius. Estimated standard deviations are 0.02 Å for bond lengths and 1.0° for bond angles.

Table IV. Peptide Backbone Conformational Angles (deg)

i	ϕ_i	ψ_i	ω_i
1	−91	129	177
2	−53	140	175
3	84	−7	−176
4	−111	119	174
5	122	179	−178

Table V. Hydrogen Bond Distances (Å) and Angles (deg)[a]

donor	hydrogen	acceptor	donor–acceptor	hydrogen–acceptor	angle
N1	H-N1	W2 a	3.00	2.05	161
	H-N1	W3 a	3.00	2.06	157
N3	H-N3	W1 a	2.91	1.94	177
N4	H-N4	O1 a	3.28	2.38	157
N5	H-N5	O2 b	3.03	2.10	168
W1		W5 a	2.57		
		W6 a	3.16		
W2		W4 a	2.97		
		O5 c	3.08		
W4		W6 a	2.74		
		O1 a	2.96		
		O4 a	2.58		
W5		O5 a	2.50		
W6		O1 a	2.86		
		O4 a	3.03		

[a] Symmetry codes: a, x, y, z; b, $^2/_3 - y, {}^4/_3 + x - y, {}^1/_3 + z$; c, $1 - y, 2 + x - y, 1 + z$.

Table IV lists the characteristic torsion angles of the peptide backbone. All linkages are within 6° of the ideal trans conformation. Furthermore, the angle pairs $\phi(2)$, $\psi(2)$ and $\phi(3)$, $\psi(3)$ for the sequence Pro-Gly fall within the range of values assigned

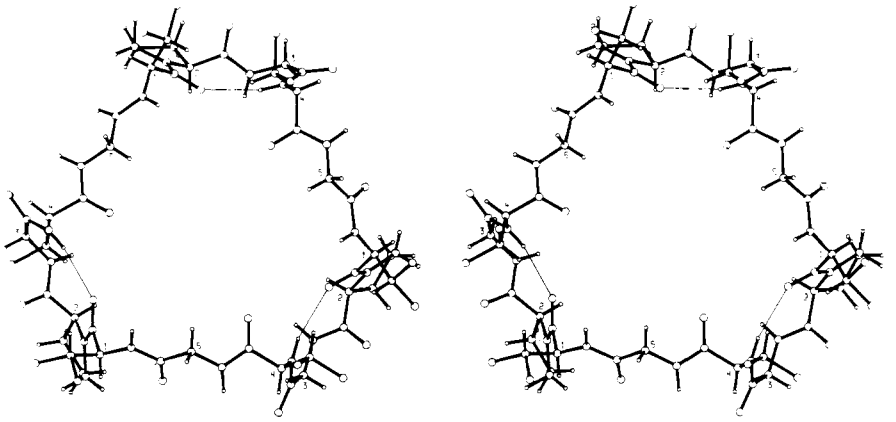

Figure 2. Stereodrawing of the trimer. The 4→1 hydrogen bond is represented by a thin line.

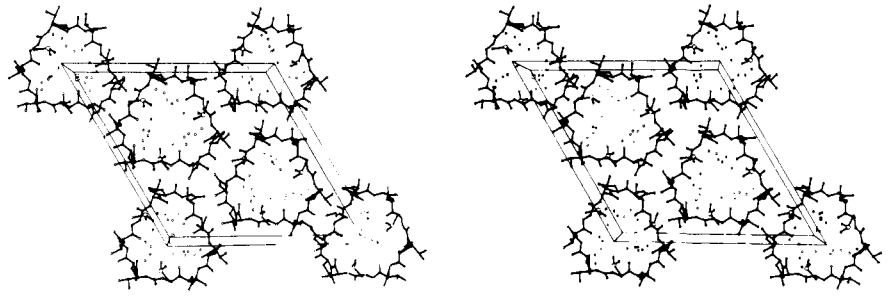

Figure 3. Stereodrawing of the crystal packing as viewed down the *c* axis.

to the β turn conformation β(II).[14,15] The intramolecular H bond associated with this structural feature is very long (weak), as may be seen in Table V, which gives distances and angles for the H bonds in the structure. This H bond, N4–H···O1, often referred to as the 4→1 H bond, shows an N···O distance of 3.28 (2) Å and an H···O distance of 2.38 Å, based on an idealized H position; these values place this 4→1 H bond near the middle of the range of analogous distances observed in β(II) turns in a variety of crystalline cyclic peptides, the majority of which are hexapeptides. In a number of the examples with longer 4→1 interactions,[16,17] close contacts between O atoms of transannular carbonyl groups impose lower limits on N···O distances. Such is not the case for the cyclic pentadecapeptide. However, as may be seen in Figure 2, which shows the entire molecule, the length of the 4→1 H bond may instead be the result of repulsions between valine side chains and of the stereochemical requirements of trimer formation. The cyclic pentadecapeptide consists of three β(II) turns joined by Val-Gly-Val bridges. These bridges are somewhat distorted from the extended conformation found in β sheets, with a ϕ_5 value (for Gly$^{(5)}$) of 122 (1)°.

Figure 3 shows a stereorepresentation of the unit cell of the cyclic pentadecapeptide crystal structure viewed down the *c* axis. Molecules are centered on the threefold axes at (0, 0, *z*), ($^1/_3$, $^2/_3$, *z*), and ($^2/_3$, $^1/_3$, *z*). Each molecule is joined to its six nearest neighbors by the only intermolecular H bond N5–H···O2. The only other bonding connection between cyclic molecules is the rather tenuous N3–W1–W5–OS–W2–N1 concatenation, which involves the sulfoxide O atom and several partially occupied water sites.

One of the most striking features of the crystal structure is the set of hydrophilic channels formed by the stacking of cyclic peptides on threefold axes. All of the solvent, so far as can be determined, is located within these channels, and the solvent that has been modeled is disposed in a triple helical fashion near the inner surface of these channels. Also to be noted are a set of hydrophobic cores running parallel to the *c* axis at (0, $^1/_3$), ($^1/_3$, 0), and ($^2/_3$, $^2/_3$) and formed by valine and proline residues, as well as another parallel set of cores at (0, $^2/_3$), ($^2/_3$, 0), and ($^1/_3$, $^1/_3$) lined with valine residues and glycyl carbonyl groups.

With the exception of W3, the solvent molecules occupy positions that would produce a reasonable structure if all positions were occupied simultaneously. W3 is 1.45 Å from W2 and 1.67 Å from W4; its presence thus excludes the latter two molecules. An attempt to refine W2 and W3 as a methanol molecule failed. The solvent that is modeled as a Me_2SO molecule of fractional occupancy is not perfectly described, as may be seen from the dimensions of the molecule: S–OS = 1.48 (4), C1S–S = 2.00 (4), and C2S–S = 1.76 (4) Å; OS–S–C1S = 105 (1), OS–S–C2S = 108 (1), and C1S–S–C2S = 108 (1)°. Nevertheless, the overall geometry of the Me_2SO model is close to that commonly observed in the solid state[18] except for the long C1S–S distance, and it is clear that solvent in this region cannot be described solely by water molecules.

In summary, the results confirm the presence of a β(II) turn in the cyclic pentadecapeptide crystal, a structural feature which was predicted for the molecule in solution from the NMR studies.[6c,19] Neither the 11-atom nor the 14-atom H-bonded ring[6c] is observed in the crystal structure. Further studies of other cyclic oligomers composed of this pentapeptide are in progress.

Acknowledgments. This research was supported by National Institutes of Health Grants CA-13148 and HL-11310.

Supplementary Material Available: Listing of structure factor amplitudes, thermal parameters of nonhydrogen atoms, and thermal parameters for hydrogen atoms (17 pages). Ordering information is given on any current masthead page.

(14) Hossain, M. B.; van der Helm, D. *J. Am. Chem. Soc.* **1978**, *100*, 5191–5198.
(15) Venkatachalam, C. M. *Biopolymers* **1968**, *6*, 1425–1436.
(16) Brown, J. N.; Teller, R. G. *J. Am. Chem. Soc.* **1976**, *98*, 7565–7569.
(17) Brown, J. N.; Yang, C. H. *J. Am. Chem. Soc.* **1979**, *101*, 445–449.
(18) Dupont, L.; Dideberg, O.; Lamotte, J.; Pielte, J. L. *Acta Crystallogr., Sect. B* **1979**, *35*, 849–852.
(19) Khaled, M. A.; Urry, D. W. *Biochem. Biophys. Res. Commun.* **1976**, *70*, 485–491.